NIH Public Access
Author Manuscript
J Pathol. Author manuscript; available in PMC 2012 March 1.

Published in final edited form as:
J Pathol. 2011 March ; 223(4): 553–565. doi:10.1002/path.2825.

Chronic Chorioamnionitis Displays Distinct Alterations of the Amniotic Fluid Proteome

Giovanna Oggé[1,†], **Roberto Romero**[1,2,3,*], **Deug-Chan Lee**[1,†], **Francesca Gotsch**[1], **Nandor Gabor Than**[1], **JoonHo Lee**[1], **Tinnakorn Chaiworapongsa**[1,2], **Zhong Dong**[1], **Pooja Mittal**[1,2], **Sonia S. Hassan**[1,2], and **Chong Jai Kim**[1,4,*]

[1] Perinatology Research Branch, NICHD/NIH/DHHS, Bethesda, Maryland, and Detroit, Michigan, USA

[2] Department of Obstetrics and Gynecology, Wayne State University School of Medicine, Detroit, Michigan, USA

[3] Center for Molecular Medicine and Genetics, Wayne State University School of Medicine, Detroit, Michigan, USA

[4] Department of Pathology, Wayne State University School of Medicine, Detroit, Michigan, USA

Abstract

Acute chorioamnionitis of infectious origin and chronic chorioamnionitis of immunologic origin are two major placental lesions of spontaneous preterm birth with elevated amniotic fluid interleukin-6 and CXCL10 concentrations, respectively. The changes in the amniotic fluid proteome associated with intra-amniotic infection and acute chorioamnionitis are well-defined, yet alterations unique to chronic chorioamnionitis remain to be elucidated. This study was conducted to determine those amniotic fluid proteins changing specifically in the presence of chronic chorioamnionitis. Amniotic fluid obtained from acute chorioamnionitis, chronic chorioamnionitis, and gestational age-matched controls were analyzed by 2-dimensional difference in gel electrophoresis and MALDI-TOF analyses. The type of histologic inflammation was used to define each condition in preterm labor cases (n=125) and term not in labor cases (n=22); and the amniotic fluid concentrations of interleukin-6, CXCL8, CXCL10, and prostaglandin $F_{2\alpha}$ were also measured by specific immunoassays. Among preterm labor cases, thirty-one differentially expressed proteins were identified in chronic chorioamnionitis cases, as compared to both acute chorioamnionitis and control cases. Importantly, glycodelin-A, which maintains maternal tolerance against an allogeneic fetus, was decreased in chronic chorioamnionitis, while haptoglobin was increased. We report the amniotic fluid proteome of chronic chorioamnionitis for the first time, and the findings herein strongly suggest that there is a pathophysiological association between the changes of immunomodulatory proteins in the amniotic fluid and chronic chorioamnionitis, a histologic manifestation of maternal anti-fetal allograft rejection.

[*]Correspondence: Chong Jai Kim, MD, PhD, Department of Pathology, Wayne State University School of Medicine, Hutzel Women's Hospital, Room 4620, 3990 John R, Detroit, MI 48201, USA. Phone: (313) 577 6404, Fax: (313) 993-2694, cjkim@med.wayne.edu. Roberto Romero, MD, Perinatology Research Branch, NICHD/NIH/DHHS, Wayne State University/Hutzel Women's Hospital, 3990 John R, Box #4, Detroit, MI 48201, USA. Phone: (313) 993-2700, Fax: (313) 993-2694, prbchiefstaff@med.wayne.edu.
[†]These authors contributed equally to this work.

The authors declare no conflicts of interest.

Author contribution statement

GO, DCL, JL, ZD, and CJK carried out experiments and analyzed the data. RR, FG, NGT, TC, PM, SSH, and CJK conceived experiments and analyzed data. All authors participated in writing the paper and approved the submitted manuscript.

NIH-PA Author Manuscript
NIH-PA Author Manuscript
NIH-PA Author Manuscript

NIH-PA Author Manuscript

NIH-PA Author Manuscript

NIH-PA Author Manuscript

Keywords

amniotic fluid; proteome; chronic chorioamnionitis; preterm birth

Introduction

Human parturition involves the activation of pro-inflammatory cascades in gestational tissues, such as the chorioamniotic membranes, in cases of spontaneous labor at term and preterm birth due to intra-amniotic infection. Not surprisingly, in both conditions there is an increased expression of prostaglandin-endoperoxide synthase 2 (PTGS2) in the chorioamniotic membranes [1–3], and the amniotic fluid prostaglandin concentrations are increased [4–7]. Acute chorioamnionitis following microbial invasion of the amniotic cavity (MIAC) is a major pathological lesion found in spontaneous preterm births (preterm labor and preterm prelabor rupture of membranes) [8–10]. However, our recent analysis demonstrated that chronic chorioamnionitis is more common in spontaneous preterm birth cases, found in 34% of preterm labor with intact membranes cases and 39% of preterm prelabor rupture of membranes cases. This lesion was also observed in 23% of term preeclampsia and 16% of preterm preeclampsia cases suggesting its link with the immunopathology of preeclampsia and indicated preterm birth as well [11,12].

Chronic chorioamnionitis, defined as the amniotropic infiltration of maternal T cells, is considered a histologic manifestation of maternal anti-fetal allograft rejection and graft-versus-host disease in the placenta [11,13,14]. Therefore, a major proportion of preterm births seems to be due to either intra-amniotic infection or allograft rejection. While amniotic fluid interleukin-6 (IL-6) is a sensitive marker of intra-amniotic infection and acute chorioamnionitis [15–17], chronic chorioamnionitis is associated with elevated intra-amniotic T cell chemokine CXC-motif ligand-10 (CXCL10) concentration and increased CXCL9, CXCL10, and CXCL11 mRNA expressions in the chorioamniotic membranes [11]. Intra-amniotic infection- and acute chorioamnionitis-associated changes in the amniotic fluid proteome have been elegantly addressed in previous studies [18–20], yet those associated with chronic chorioamnionitis remain to be elucidated. The assessment of changes in the amniotic fluid proteome could unveil key alterations in the intra-amniotic environment leading to the development of chronic chorioamnionitis and preterm birth. This study was conducted to determine specific changes in the abundance of amniotic fluid proteins in the presence of chronic chorioamnionitis.

Materials and methods

Patient materials

This cross-sectional study included 125 women with a singleton pregnancy who presented with preterm labor with intact membranes and 22 women with normal pregnancy at term not in labor. The study was approved by the Institutional Review Boards of participating institutions, and all participants provided written informed consent for the collection of biological materials and clinical data. Amniotic fluid samples were obtained by transabdominal amniocentesis performed to assess the microbial status of the amniotic cavity or fetal lung maturity. Histologic diagnosis of placental lesions was done by examination of hematoxylin and eosin stained sections of the chorioamniotic membranes (n=1), placental disc (n=2), and umbilical cord (n=1) in each case. The diagnosis of acute chorioamnionitis was made based on the criteria previously described [21]. The diagnosis of chronic chorioamnionitis was made when lymphocytic infiltration into the chorionic trophoblast layer or chorioamniotic connective tissue was observed. The extent of chronic chorioamnionitis was graded 1 when there were more than two foci or patchy inflammation,

NIH-PA Author Manuscript

NIH-PA Author Manuscript

NIH-PA Author Manuscript

and 2 when diffuse inflammation was present. The stage of inflammation was scored as 1 if amniotropic lymphocytic infiltration was limited to the chorionic trophoblast layer, and 2 if lymphocytic infiltration extended into the chorioamniotic connective tissue [11].

Enzyme-linked immunosorbent assay (ELISA)

The amniotic fluid concentrations of IL-6 (R&D Systems, Minneapolis, MN, USA), CXCL8 (R&D Systems), CXCL10 (R&D Systems), $PGF_{2\alpha}$ (Assay Designs, Inc., Ann Arbor, MI, USA), and glycodelin-A (DRG Diagnostics, Marburg, Germany) were measured by specific immunoassays according to the manufacturers' instructions.

2-Dimensional Difference in Gel Electrophoresis (2D-DIGE)

Three gestational age-matched amniotic fluid samples of each histologic group [no inflammation-control (gestational age: 24.9, 27.4, 33.4 weeks), acute chorioamnionitis (gestational age: 25.3, 27.4, 33.4 weeks), chronic chorioamnionitis (gestational age: 25.1, 28.9, 33.9 weeks)] were selected. These three samples were then pooled to represent each group. Methanol was added to the pooled amniotic fluid samples (volume ratio 9:1), and the precipitated proteins were resolubilized in lysis buffer [30 mM Tris-HCl (pH 8.8), 7 M urea, 2 M thiourea, 4% CHAPS]. Thirty μg of proteins from each pooled sample were labeled with Cy2, Cy3, and Cy5, respectively. The labeling reaction was stopped by adding 1.0 ul of 10 mM Lysine to each sample, and incubating in the dark on ice for an additional 15 min. The labeled samples were then mixed with 2X sample buffer [8 M urea, 4% CHAPS, 20 mg/ml dithiothreitol (DTT), 2% pharmalytes] and 100 μl destreak rehydration buffer (7 M urea, 2 M thiourea, 4% CHAPS, 20 mg/ml DTT, 1% pharmalytes) to make a total volume of 250 μl. The samples were mixed, spun, and then loaded into a strip holder. After isoelectric focusing (pH 3–10), IPG strips were incubated in equilibration buffer-1 (50 mM Tris-HCl, pH 8.8, 6 M urea, 30% glycerol, 2% SDS, 10 mg/ml DTT) for 15 min with gentle shaking, and then rinsed in equilibration buffer-2 [50 mM Tris-HCl (pH 8.8), 6 M urea, 30% glycerol, 2% SDS, 45 mg/ml DTT] for 10 min with gentle shaking. Following electrophoresis in a 12% SDS-polyacrylamide gel at 15°C, the gel was scanned using Typhoon TRIO (Amersham BioSciences, Piscataway, NJ, USA). Scanned images were then analyzed by Image Quant software version 6.0 (Amersham BioSciences), followed by differential in-gel analysis using DeCyder software version 6.5 (GE Healthcare, Piscataway, NJ, USA), to obtain the fold-changes in protein expression.

Mass Spectrometry

The spots of interest were picked up by Ettan Spot Picker (Amersham BioSciences) and digested in-gel with modified porcine trypsin protease (Trypsin Gold; Promega, Madison, WI, USA). The digested tryptic peptides were desalted by Zip-tip C18 (Millipore, Billerica, MA, USA). Peptides were eluted from the Zip-tip with 0.5 μl of matrix solution (5 mg/ml of α-cyano-4-hydroxycinnamic acid in 50% acetonitrile, 0.1% trifluoroacetic acid, 25 mM ammonium bicarbonate) and spotted on the MALDI plate (model ABI 01-192-6-AB). MALDI-TOF and TOF/TOF mass spectrometry were performed on an ABI 4700 mass spectrometer (Applied Biosystems, Framingham, MA, USA). MALDI-TOF mass spectra were acquired in reflectron-positive ion mode, averaging 4000 laser shots per spectrum. TOF/TOF mass spectrometry fragmentation spectra were acquired for each sample, averaging 4000 laser shots per fragmentation spectrum on each of the 10 most abundant ions present in each sample. Both the resulting peptide mass and the associated fragmentation spectra were submitted to a GPS Explorer workstation equipped with a MASCOT search engine (Matrix Science Ltd., London, United Kingdom) to search the redundant database of the National Center for Biotechnology Information (NCBInr). Searches were performed without constraining protein molecular weight or isoelectric point, with variable carbamidomethylation of cysteine and oxidation of methionine residues, and with one

NIH-PA Author Manuscript

NIH-PA Author Manuscript

NIH-PA Author Manuscript

missed cleavage also allowed in the search parameters. Candidates with either a protein score of C.I.% or Ion C.I.% greater than 95 were considered significant.

Immunoblotting

Immunoblotting for haptoglobin was done using 3.5 μl of amniotic fluid. Electrophoresis was done under reducing conditions in 12% SDS-PAGE, and proteins were electro-blotted onto polyvinylidene difluoride membranes. The membranes were incubated with mouse monoclonal anti-haptoglobin-beta antibody (Santa Cruz Biotechnology Inc., Santa Cruz, CA, USA), and then with HRP-conjugated anti-mouse IgG. Chemiluminescence was detected using a ChemiGlow West kit (Alpha Innotech Corporation, San Leandro, CA, USA). β-haptoglobin density was analyzed by FluorChem™ SP densitometry using AlphaEase®FC Software (Version 4.1.0; Alpha Innotech Corporation).

Immunohistochemistry

Formalin-fixed, paraffin-embedded 5-μm-thick tissue sections of the chorioamniotic membranes obtained from preterm labor cases without inflammation (n=5), with acute chorioamnionitis (n=5), and chronic chorioamnionitis (n=5) were used for immunostaining using a Ventana Discovery automatic staining system (Ventana Medical Systems, Tucson, AZ, USA). Immunostaining was performed using a mouse monoclonal anti-CD8 antibody (1:100 diluted, Dako, Carpinteria, CA, USA), a rabbit monoclonal anti-pregnancy-associated endometrial alpha-2 globulin (PAEP, glycodelin-A) antibody (1:100 diluted, Life Span Biosciences, Inc., Seattle, WA, USA), and a mouse monoclonal anti-haptoglobin beta antibody (1:100 diluted, Santa Cruz Biotechnology Inc.). Chromogen reaction was done using the DiscoveryR DAB Map Kit (Ventana Medical Systems).

Statistical analysis

Normality of the data distribution was tested using the Kolmogorov-Smirnov test. Comparisons among the study groups were performed by the unpaired *t*-test and *post hoc* analysis or Kruskall-Wallis test and Mann-Whitney *U*-test for continuous variables, as well as by the χ^2-test and Fisher's exact test for categorical variables as appropriate. Spearman rank correlation was used to examine the relationship of $PGF_{2\alpha}$ concentration with IL-6 and with CXCL10 concentrations in amniotic fluid and between glycodelin-A concentration and gestational age. A p value of < 0.05 was considered significant.

Results

Amniotic fluid IL-6, CXCL8, CXCL10, and $PGF_{2\alpha}$

The demographics and clinical characteristics of the study population are shown in Table 1, and histological and immunohistochemical features of each group are shown in Figures 1A–1F. Amniotic fluid cultures for aerobes, anaerobes and Mycoplasmas were available in all preterm labor cases. Among 71 cases without inflammation (control), one case had a positive culture. Amniotic fluid cultures were positive in four of the 14 cases of acute chorioamnionitis (28.6%). Cultures were negative in all chronic chorioamnionitis cases (n=40). To further characterize acute chorioamnionitis and chronic chorioamnionitis cases, amniotic fluid IL-6, CXCL8, CXCL10, and $PGF_{2\alpha}$ concentrations were measured by immunoassay.

The median IL-6 concentration was higher in acute chorioamnionitis cases (median: 7.2 ng/ml, range: 0.4–388.9 ng/ml) than in chronic chorioamnionitis cases (median 0.6 ng/ml, range 0.1–15.2 ng/ml; p=0.002) or in control cases (median: 0.6 ng/ml, range: 0.0–14.8 ng/ml; p=0.001) (Figure 2A). Among acute chorioamnionitis cases, IL-6 concentration was significantly higher in those with positive amniotic fluid culture compared to those with

NIH-PA Author Manuscript

NIH-PA Author Manuscript

NIH-PA Author Manuscript

negative culture (median 217.3, range 18.5–388.9 ng/ml vs. median 1.0, range 0.4–241.1 ng/ml; p=0.014). Using a concentration cut-off of 12.4 ng/ml identified with a receiver-operating characteristic (ROC) curve (area under the curve (AUC): 0.979; 95% CI: 0.931–1.027; p<0.001), IL-6 had sensitivity, specificity, positive predictive value, and negative predictive value of 100%, 87.5%, 66.7% and 100%, respectively, for acute chorioamnionitis in patients who delivered within seven days of amniocentesis.

The median concentration of CXCL8 was significantly higher in acute chorioamnionitis cases (median 3.4 ng/ml, range: 0.1–467.0 ng/ml) than in chronic chorioamnionitis cases (median 0.5 ng/ml, range: 0.1–15.7 ng/ml; p=0.048) or in control cases (median 0.4 ng/ml, range: 0.1–14.8 ng/ml; p=0.019) (Figure 2B).

The median amniotic fluid CXCL10 concentration was higher in chronic chorioamnionitis cases (median: 2.7 ng/ml, range: 0.0–20.8 ng/ml) than in the acute chorioamnionitis cases (median: 1.1 ng/ml, range: 0.4–4.5 ng/ml; p=0.02) and the control cases (median: 1.1 ng/ml, range: 0.0–5.8 ng/ml; p<0.001) (Figure 2C). Using a concentration cut-off of 1.1 ng/ml identified with a ROC curve (AUC: 0.769; 95% CI 0.643–0.895; p=0.001), CXCL10 had sensitivity, specificity, positive predictive value, and negative predictive value of 85.7%, 61%, 52.9% and 89.3%, respectively, for chronic chorioamnionitis in patients delivering within 28 days of amniocentesis.

Preterm labor due to intra-amniotic infection is characterized by increased prostaglandin concentrations in the amniotic fluid [4–7,22]. To determine whether chronic chorioamnionitis shows comparable changes in the amniotic fluid prostaglandins, $PGF_{2\alpha}$ was also measured. The median amniotic fluid concentration of $PGF_{2\alpha}$ was significantly higher in cases with acute chorioamnionitis (median: 101.2 ng/ml, range: 2.4–2216.4 ng/ml) compared to both chronic chorioamnionitis cases (median: 40.2 ng/ml, range: 6.7–514.6 ng/ml; p=0.02) and control cases (median: 36.1 ng/ml, range: 1.9–1565.8 ng/ml; p=0.01), while no differences were observed between chronic chorioamnionitis and control cases (Figure 2D). Among acute chorioamnionitis cases, $PGF_{2\alpha}$ concentration tended to be higher in cases with positive culture (median 704.8, range 183.4–2216.4 pg/ml vs. median 54.7, range2.4–939.9 pg/ml; p=0.05). Amniotic fluid $PGF_{2\alpha}$ concentration showed a moderate correlation with that of IL-6 (Spearman rho coefficient: 0.384, p<0.001) but not with CXCL10 (Spearman rho coefficient: 0.062, p=0.5).

The amniotic fluid concentrations of IL-6 (median 0.5 ng/ml, range 0.2–1.8 ng/ml; Figure 3A), and CXCL10 (median 0.8 ngml, range 0.1–6.0 ng/ml Figure 3C) of normal pregnant women at term were not different from those of preterm labor cases without histologic inflammation. However, CXCL8 concentration (median 1.0 ng/ml, range 0.3–.3.9 ng/ml; Figure 3B) and $PGF_{2\alpha}$ concentration (median 155.3 pg/ml, range 11.8–1338.5 pg/ml; Figure 3D) of term cases were significantly higher than that of preterm labor cases (p=0.003 and p<0.001 respectively).

2D-DIGE of Amniotic Fluid

Figure 4A shows the 2-D electrophoresis gel with 71 spots showing differentially expressed proteins amongst the three groups. Differentially expressed spots with more than 2-fold changes in chronic chorioamnionitis compared to acute chorioamnionitis or control cases were analyzed (Figure 4B). Table 2 provides the list of 31 differentially expressed proteins identified from 41 spots in 2D-DIGE analysis of pooled amniotic fluid samples from the three groups (control, acute chorioamnionitis, and chronic chorioamnionitis). Several acute phase proteins such as α-1-antichymotrypsin, α-1-antitrypsin, and haptoglobin were increased in chronic chorioamnionitis. Several plasma proteins were also differentially represented in chronic chorioamnionitis: plasminogen and transferrin were increased, while

NIH-PA Author Manuscript

NIH-PA Author Manuscript

NIH-PA Author Manuscript

ceruloplasmin was decreased. Orosomucoid 2 and insulin-like growth factor binding protein 1 precursor were decreased in chronic chorioamnionitis compared to the controls but did not change in acute chorioamnionitis. Interestingly, glycodelin-A was 6.1-fold and 5.5-fold reduced in chronic chorioamnionitis compared to acute chorioamnionitis and controls, respectively.

To confirm the results of 2D-DIGE, amniotic fluid glycodelin-A concentration was measured by immunoassay. When all results from the cases were analyzed, there was no difference among the groups ($p = 0.2$). When examining cases ≤ 32 weeks of gestation ($n = 68$), however, based on the fact that amniotic fluid glycodelin-A concentration rapidly decreases by the end of the second trimester [23], and that two out of three amniotic fluid samples used for 2D-DIGE were obtained before 29 weeks of gestation, median amniotic fluid glycodelin-A concentration was significantly lower in chronic chorioamnionitis cases (median: 1639.9 ng/ml, range: 45.2–12718.0 ng/ml) compared to control cases (median: 3184.3 ng/ml, range: 28.3–97991.2 ng/ml; $p < 0.05$) (Figure 5A). Glycodelin-A concentration in acute chorioamnionitis cases (median: 3166.8 ng/ml, range: 278.9–55608.1 ng/ml) also tended to be higher than that found in chronic chorioamnionitis cases ($p = 0.091$). Such differences were not present in samples collected after 32 weeks ($p = 0.9$). This seems to be associated with a marked physiological decrease in amniotic fluid glycodelin-A concentration. Indeed, there was a significant negative correlation between glycodelin-A concentration and gestational age at amniocentesis (Spearman rho coefficient = −0.479; $p < 0.001$). Even when the controls were divided into high and low amniotic fluid glycodelin-A using median concentration as the cut-off value, the gestational age of low glycodelin-A cases (median: 30.4 weeks, range: 26.6 – 32.0 weeks) was significantly higher than that of high glycodelin-A cases (median: 27.4 weeks, range: 22.7 – 31.7 weeks). However, there was no difference in gestational age between control and chronic chorioamnionitis cases, indicating that decreased amniotic fluid glycodelin-A concentration is a feature of chronic chorioamnionitis.

The differences in the amniotic fluid concentration of haptoglobin observed by 2D-DIGE were further assessed by immunoblotting in a subgroup of samples associated with isolated acute chorioamnionitis ($n = 11$), chronic chorioamnionitis ($n = 16$), and control cases ($n = 16$). Densitometric analysis of the immunoblotting results was performed. The abundance of the β-subunit of haptoglobin in the amniotic fluid of cases collected at ≤ 32 weeks of gestation ($n = 23$) was higher in chronic chorioamnionitis cases (median sample haptoglobin/pooled sample haptoglobin ratio: 2.9, range: 0.4 – 4.1) compared to both acute chorioamnionitis cases (median sample haptoglobin/pooled sample haptoglobin ratio: 0.6, range: 0.4 – 2.3, $p<0.05$) and control cases (median sample haptoglobin/pooled sample haptoglobin ratio: 0.7, range: 0.3–2.3, $p<0.05$) (Figure 5B, 5C), while the difference was not observed in cases > 32 weeks of gestation ($n = 20$), as was the case with glycodelin-A.

Glycodelin-A and Haptoglobin Immunoreactivity in the Chorioamniotic Membranes

For the localization of glycodelin-A and haptoglobin expression, sections of the chorioamniotic membranes were immunostained for glycodelin-A and haptoglobin. Intense cytoplasmic glycodelin-A immunoreactivity was found in the endometrial epithelial cells. On the other hand, decidual stromal cells showed a predominantly membranous staining pattern (Figure 6A and 6B). Haptoglobin immunoreactivity was localized in the cytoplasm of decidual leukocytes, and also in the cytoplasm of myofibroblasts and macrophages in the chorioamniotic connective tissue (Figure 6C and 6D). Neutrophil infiltrates in acute chorioamnionitis were also weakly immunoreactive.

NIH-PA Author Manuscript

NIH-PA Author Manuscript

NIH-PA Author Manuscript

Discussion

The primary findings of this study are: 1) There are changes in the amniotic fluid proteome unique to chronic chorioamnionitis compared to acute chorioamnionitis or no inflammation cases; and, 2) Acute chorioamnionitis and chronic chorioamnionitis are different in terms of the changes in amniotic fluid IL-6, CXCL8, CXCL10, and $PGF_{2\alpha}$ concentrations. The changes in amniotic fluid chemokine concentrations (CXCL8, CXCL10) were consistent with amniotropic infiltration patterns of maternal/fetal neutrophils and maternal T cells in acute chorioamnionitis and chronic chorioamnionitis, respectively. These observations further support the fact that acute chorioamnionitis and chronic chorioamnionitis are manifestations of different pathological processes, particularly in the mechanisms leading to preterm labor.

Among the changes in amniotic fluid proteome associated with chronic chorioamnionitis, decreased glycodelin-A concentration is particularly intriguing. Glycodelin, also known as progesterone-associated endometrial protein, placental protein 14, and progestagen-dependent endometrial protein, is a dimeric glycoprotein belonging to the lipocalin family [23,24]. At least four isoforms of identical amino acid sequence but with different oligosaccharide structures and biological functions are present: glycodelin-A was isolated from the amniotic fluid [25], glycodelin-F from the follicular fluid [26], glycodelin-C from the extracellular matrix of the cumulus oophorus [27], and glycodelin-S from epithelial cells of the seminal glands [28]. The most abundant isoform in the female reproductive tract is glycodelin-A, which is produced by endometrial and decidual epithelial cells and secreted in the endometrial fluid and amniotic fluid and into the circulation [24,29]. Glycodelin-A has two main functions: contraceptive activity due to the inhibition of the binding of spermatozoa to the zona pellucida [30], and immunosuppression. The immunosuppressive activity is mediated by several different mechanisms and is effective on all predominant immune cell lineages at the maternal-fetal interface: lymphocytes, monocytes, and natural killer cells.

T cells are the most well-defined target of the immunosuppressive action of glycodelin-A. The proliferative response of T lymphocytes to allogeneic stimulation [31] and to phytohemagglutinin [32] is inhibited by glycodelin-A in a dose-dependent manner. This property is dependent on interaction with CD45, a tyrosine phosphatase with regulatory activity on the T cell receptor signaling pathway, which results in an elevation of the T cell receptor activation threshold [33]. While both Th1 and Th2 responses are inhibited by glycodelin-A, the Th1 differentiation pathway is more sensitive to the inhibition of T cell receptor signaling, thus leading an overall shift toward Th2 differentiation [34]. Moreover, glycodelin-A induces apoptosis of activated T cells [35] by an intrinsic pathway [36]. The cell receptor (or one of the receptors) responsible for its apoptotic activity on T cells was shown to be CD7, a galactose-containing surface glycoprotein expressed in activated T cells. CD7 is also recognized by galectin-1 and galectin-3 [37]. Glycodelin-A also inhibits monocyte chemotaxis [38] and induces monocyte apoptosis via the intrinsic mitochondrial stress-induced pathway [39]. Furthermore, glycodelin-A can inhibit the cytotoxic activity of circulating natural killer cells [40], possibly through induction of an apoptotic cascade which, unlike for T cells and monocytes, does not involve the mitochondrial pathway [39].

Because of its abundance at the maternal-fetal interface, it was suggested that glycodelin-A maintains maternal immune tolerance against fetal allo-antigens [39]. Indeed, a large body of evidence supports an important role for glycodelin-A in the maintenance of physiologic pregnancy: 1) women with unexplained infertility have a lower glycodelin-A concentration in uterine flushing [41]; 2) uterine fluid and serum glycodelin-A concentrations are reduced in women with a history of recurrent miscarriage [42,43]; 3) glycodelin-A expression is

NIH-PA Author Manuscript

NIH-PA Author Manuscript

NIH-PA Author Manuscript

reduced in decidual tissues from first-trimester spontaneous abortions compared to normal pregnancies [44]; and 4) reduced decidual expression of glycodelin-A has been reported in pregnancies complicated with preeclampsia, HELLP syndrome, and fetal growth restriction, compared to normal pregnancies [45]. Our observation that amniotic fluid glycodelin-A concentration is decreased in chronic chorioamnionitis is novel. This strongly suggests that the impairment of a physiologic constraint of the maternal immune system against fetal antigens is associated with and precedes the development of chronic chorioamnionitis.

Glycodelin-A production and release are under hormonal control, as it is up-regulated by progesterone [46], with estrogen exerting a priming effect [47]; human chorionic gonadotrophin (hCG) also stimulates glycodelin-A expression in endometrial cells [48], while glycodelin-A induces hCG expression by the cytotrophoblasts [49]. The concentration of glycodelin-A in the amniotic fluid, as well as in the maternal serum, is known to vary with gestational age. Amniotic fluid concentration of glycodelin-A increases during early pregnancy to peak at 15–16 weeks of gestation, and then it rapidly drops until 19 weeks, has a temporary elevation around 23 weeks, and finally decreases until term [23,50]. A significant correlation between glycodelin-A concentration and gestational age was also confirmed in this study. Taken together, the elevation in T cell chemokine CXCL10 concentration and the decreased concentration of the T cell suppressor glycodelin-A in the amniotic fluid are consistent with the notion that a derangement of the mechanisms governing maternal immune tolerance toward the semi-allogeneic fetus is involved in the pathogenesis of chronic chorioamnionitis [11].

This study also identified a set of proteins that were differentially expressed in amniotic fluid associated with chronic chorioamnionitis cases compared to acute chorioamnionitis cases or control cases, suggesting chronic chorioamnionitis as a distinct pathological process. Many of these proteins, such as α 1-antitrypsin, α1-antichymotrypsin, haptoglobin, ceruloplasmin, and orosomucoid 2 are known as acute phase proteins [51]. These are mainly, but not exclusively, produced by hepatocytes in response to pro-inflammatory stimuli, such as infections, trauma, tissue infarction, and cancer [51]. The origin and the role of these proteins in the amniotic fluid are not yet known; however, they are likely to serve several functions besides the modulation of the acute inflammatory process. Haptoglobin, for instance, inhibits T cell response to phytohemagglutinin [52,53], B-cell response to lipopolysaccharide [54,55] and the release of T helper 2 cytokines IL-4, IL-5, IL-13, and IL-10 [53]. Moreover, haptoglobin acts as an adipokine with chemotactic action toward monocytes-macrophages in white adipose tissue [56]. It is therefore plausible that haptoglobin and other acute phase proteins present in the amniotic fluid are involved in the immunologic regulation of maternal-fetal interactions, although their roles have yet to be explored.

In summary, we report unique changes in the amniotic fluid proteome associated with chronic chorioamnionitis for the first time, and propose that acute chorioamnionitis and chronic chorioamnionitis comprise two major clusters of spontaneous preterm births having distinct perturbations in the intra-amniotic protein environment. While acute chorioamnionitis is a result of microbial invasion of the amniotic cavity and intrauterine infection [57,58], chronic chorioamnionitis could be a consequence of derangement of the hormone immune system (progesterone, glycodelin-A) affecting CD8+ T cell activity [59]. The findings herein strongly suggest that compromised tolerogenic pressure in the intrauterine environment leads to maternal anti-fetal rejection in the form of chronic chorioamnionitis in the chorioamniotic membranes.

NIH-PA Author Manuscript

NIH-PA Author Manuscript

NIH-PA Author Manuscript

Acknowledgments

This work was supported (in part) by the Perinatology Research Branch, Division of Intramural Research, *Eunice Kennedy Shriver* National Institute of Child Health and Human Development, NIH, DHHS. The authors would like to thank Dr. Hongjin Huang for her excellent technical support in proteomic analysis. The authors are grateful to the patients who agreed to participate in our studies, the nurses, laboratory staff, and clinicians who made this work possible.

Reference List

1. Fuentes A, Spaziani EP, O'Brien WF. The expression of cyclooxygenase-2 (COX-2) in amnion and decidua following spontaneous labor. Prostaglandins. 1996; 52:261–267. [PubMed: 8936582]
2. Slater D, Dennes W, Sawdy R, et al. Expression of cyclo-oxygenase types-1 and -2 in human fetal membranes throughout pregnancy. J Mol Endocrinol. 1999; 22:125–130. [PubMed: 10194515]
3. Allport VC, Pieber D, Slater DM, et al. Human labour is associated with nuclear factor-kappaB activity which mediates cyclo-oxygenase-2 expression and is involved with the 'functional progesterone withdrawal'. Mol Hum Reprod. 2001; 7:581–586. [PubMed: 11385114]
4. Dray F, Frydman R. Primary prostaglandins in amniotic fluid in pregnancy and spontaneous labor. Am J Obstet Gynecol. 1976; 126:13–19. [PubMed: 961739]
5. Romero R, Emamian M, Wan M, et al. Prostaglandin concentrations in amniotic fluid of women with intra-amniotic infection and preterm labor. Am J Obstet Gynecol. 1987; 157:1461–1467. [PubMed: 3480691]
6. Romero R, Munoz H, Gomez R, et al. Increase in prostaglandin bioavailability precedes the onset of human parturition. Prostaglandins Leukot Essent Fatty Acids. 1996; 54:187–191. [PubMed: 8860106]
7. Lee SE, Romero R, Park IS, et al. Amniotic fluid prostaglandin concentrations increase before the onset of spontaneous labor at term. J Matern Fetal Neonatal Med. 2008; 21:89–94. [PubMed: 18240075]
8. Gray DJ, Robinson HB, Malone J, et al. Adverse outcome in pregnancy following amniotic fluid isolation of Ureaplasma urealyticum. Prenat Diagn. 1992; 12:111–117. [PubMed: 1553356]
9. Horowitz S, Mazor M, Romero R, et al. Infection of the amniotic cavity with Ureaplasma urealyticum in the midtrimester of pregnancy. J Reprod Med. 1995; 40:375–379. [PubMed: 7608879]
10. Novy MJ, Duffy L, Axthelm MK, et al. Ureaplasma parvum or Mycoplasma hominis as sole pathogens cause chorioamnionitis, preterm delivery, and fetal pneumonia in rhesus macaques. Reprod Sci. 2009; 16:56–70. [PubMed: 19122105]
11. Kim CJ, Romero R, Kusanovic JP, et al. The frequency, clinical significance, and pathological features of chronic chorioamnionitis: a lesion associated with spontaneous preterm birth. Mod Pathol. 2010; 23:1000–1011. [PubMed: 20348884]
12. Redman CW, Sargent IL. Immunology of pre-eclampsia. Am J Reprod Immunol. 2010; 63:534–543. [PubMed: 20331588]
13. Gersell DJ, Phillips NJ, Beckerman K. Chronic chorioamnionitis: a clinicopathologic study of 17 cases. Int J Gynecol Pathol. 1991; 10:217–229. [PubMed: 1917272]
14. Jacques SM, Qureshi F. Chronic chorioamnionitis: a clinicopathologic and immunohistochemical study. Hum Pathol. 1998; 29:1457–1461. [PubMed: 9865833]
15. Romero R, Avila C, Santhanam U, et al. Amniotic fluid interleukin 6 in preterm labor. Association with infection. J Clin Invest. 1990; 85:1392–1400. [PubMed: 2332497]
16. Romero R, Yoon BH, Mazor M, et al. The diagnostic and prognostic value of amniotic fluid white blood cell count, glucose, interleukin-6, and gram stain in patients with preterm labor and intact membranes. Am J Obstet Gynecol. 1993; 169:805–816. [PubMed: 7694461]
17. Andrews WW, Hauth JC, Goldenberg RL, et al. Amniotic fluid interleukin-6: correlation with upper genital tract microbial colonization and gestational age in women delivered after spontaneous labor versus indicated delivery. Am J Obstet Gynecol. 1995; 173:606–612. [PubMed: 7645642]

NIH-PA Author Manuscript

NIH-PA Author Manuscript

NIH-PA Author Manuscript

18. Gravett MG, Novy MJ, Rosenfeld RG, et al. Diagnosis of intra-amniotic infection by proteomic profiling and identification of novel biomarkers. JAMA. 2004; 292:462–469. [PubMed: 15280344]
19. Romero R, Kusanovic JP, Gotsch F, et al. Isobaric labeling and tandem mass spectrometry: a novel approach for profiling and quantifying proteins differentially expressed in amniotic fluid in preterm labor with and without intra-amniotic infection/inflammation. J Matern Fetal Neonatal Med. 2010; 23:261–280. [PubMed: 19670042]
20. Buhimschi IA, Zambrano E, Pettker CM, et al. Using proteomic analysis of the human amniotic fluid to identify histologic chorioamnionitis. Obstet Gynecol. 2008; 111:403–412. [PubMed: 18238979]
21. Redline RW, Heller D, Keating S, et al. Placental diagnostic criteria and clinical correlation--a workshop report. Placenta. 2005; 26:S114–S117. [PubMed: 15837060]
22. Lee SE, Park IS, Romero R, et al. Amniotic fluid prostaglandin F2 increases even in sterile amniotic fluid and is an independent predictor of impending delivery in preterm premature rupture of membranes. J Matern Fetal Neonatal Med. 2009; 22:880–886. [PubMed: 19544157]
23. Than, GN.; Bohn, H.; Szabo, DG. Advances in pregnancy-related protein research: functional and clinical applications. CRC Press Inc; Boca Raton FL: 1993. p. 1-333.
24. Seppala M, Taylor RN, Koistinen H, et al. Glycodelin: a major lipocalin protein of the reproductive axis with diverse actions in cell recognition and differentiation. Endocr Rev. 2002; 23:401–430. [PubMed: 12202458]
25. Riittinen L, Julkunen M, Seppala M, et al. Purification and characterization of endometrial protein PP14 from mid-trimester amniotic fluid. Clin Chim Acta. 1989; 184:19–29. [PubMed: 2688994]
26. Tse JY, Chiu PC, Lee KF, et al. The synthesis and fate of glycodelin in human ovary during folliculogenesis. Mol Hum Reprod. 2002; 8:142–148. [PubMed: 11818517]
27. Chiu PC, Chung MK, Koistinen R, et al. Cumulus oophorus-associated glycodelin-C displaces sperm-bound glycodelin-A and -F and stimulates spermatozoa-zona pellucida binding. J Biol Chem. 2007; 282:5378–5388. [PubMed: 17192260]
28. Julkunen M, Wahlstrom T, Seppala M, et al. Detection and localization of placental protein 14-like protein in human seminal plasma and in the male genital tract. Arch Androl. 1984; 12 (Suppl):59–67. [PubMed: 6398989]
29. Seppala M. Advances in uterine protein research: reproduction and cancer. Int J Gynaecol Obstet. 2004; 85:105–118. [PubMed: 15099771]
30. Oehninger S, Coddington CC, Hodgen GD, et al. Factors affecting fertilization: endometrial placental protein 14 reduces the capacity of human spermatozoa to bind to the human zona pellucida. Fertil Steril. 1995; 63:377–383. [PubMed: 7531163]
31. Bolton AE, Pockley AG, Clough KJ, et al. Identification of placental protein 14 as an immunosuppressive factor in human reproduction. Lancet. 1987; 1:593–595. [PubMed: 2881133]
32. Pockley AG, Bolton AE. Placental protein 14 (PP14) inhibits the synthesis of interleukin-2 and the release of soluble interleukin-2 receptors from phytohaemagglutinin-stimulated lymphocytes. Clin Exp Immunol. 1989; 77:252–256. [PubMed: 2789118]
33. Rachmilewitz J, Borovsky Z, Riely GJ, et al. Negative regulation of T cell activation by placental protein 14 is mediated by the tyrosine phosphatase receptor CD45. J Biol Chem. 2003; 278:14059–14065. [PubMed: 12556471]
34. Mishan-Eisenberg G, Borovsky Z, Weber MC, et al. Differential regulation of Th1/Th2 cytokine responses by placental protein 14. J Immunol. 2004; 173:5524–5530. [PubMed: 15494501]
35. Mukhopadhyay D, Sundereshan S, Rao C, et al. Placental protein 14 induces apoptosis in T cells but not in monocytes. J Biol Chem. 2001; 276:28268–28273. [PubMed: 11325960]
36. SundarRaj S, Mukhopadhyay D, Karande AA. Glycodelin A triggers mitochondrial stress and apoptosis in T cells by a mechanism distinct and independent of TCR signaling. Mol Immunol. 2008; 45:2391–2400. [PubMed: 18155767]
37. SundarRaj S, Soni C, Karande AA. Glycodelin A triggers T cell apoptosis through a novel calcium-independent galactose-binding lectin activity. Mol Immunol. 2009; 46:3411–3419. [PubMed: 19683346]

NIH-PA Author Manuscript

NIH-PA Author Manuscript

NIH-PA Author Manuscript

38. Vigne JL, Hornung D, Mueller MD, et al. Purification and characterization of an immunomodulatory endometrial protein, glycodelin. J Biol Chem. 2001; 276:17101–17105. [PubMed: 11278680]
39. Alok A, Mukhopadhyay D, Karande AA. Glycodelin A, an immunomodulatory protein in the endometrium, inhibits proliferation and induces apoptosis in monocytic cells. Int J Biochem Cell Biol. 2009; 41:1138–1147. [PubMed: 18996219]
40. Okamoto N, Uchida A, Takakura K, et al. Suppression by human placental protein 14 of natural killer cell activity. Am J Reprod Immunol. 1991; 26:137–142. [PubMed: 1840727]
41. Mackenna A, Li TC, Dalton C, et al. Placental protein 14 levels in uterine flushing and plasma of women with unexplained infertility. Fertil Steril. 1993; 59:577–582. [PubMed: 8458460]
42. Tulppala M, Julkunen M, Tiitinen A, et al. Habitual abortion is accompanied by low serum levels of placental protein 14 in the luteal phase of the fertile cycle. Fertil Steril. 1995; 63:792–795. [PubMed: 7890064]
43. Dalton CF, Laird SM, Estdale SE, et al. Endometrial protein PP14 and CA-125 in recurrent miscarriage patients; correlation with pregnancy outcome. Hum Reprod. 1998; 13:3197–3202. [PubMed: 9853880]
44. Toth B, Roth K, Kunert-Keil C, et al. Glycodelin protein and mRNA is downregulated in human first trimester abortion and partially upregulated in mole pregnancy. J Histochem Cytochem. 2008; 56:477–485. [PubMed: 18256018]
45. Jeschke U, Kunert-Keil C, Mylonas I, et al. Expression of glycodelin A in decidual tissue of preeclamptic, HELLP and intrauterine growth-restricted pregnancies. Virchows Arch. 2005; 446:360–368. [PubMed: 15756591]
46. Taylor RN, Savouret JF, Vaisse C, et al. Promegestone (R5020) and mifepristone (RU486) both function as progestational agonists of human glycodelin gene expression in isolated human epithelial cells. J Clin Endocrinol Metab. 1998; 83:4006–4012. [PubMed: 9814484]
47. Li TC, Dalton C, Bolton AE, et al. An analysis of the variation of plasma concentrations of placental protein 14 in artificial cycles. Fertil Steril. 1992; 57:776–782. [PubMed: 1555688]
48. Jeschke U, Toth B, Scholz C, et al. Glycoprotein and carbohydrate binding protein expression in the placenta in early pregnancy loss. J Reprod Immunol. 2010; 85:99–105. [PubMed: 20299109]
49. Jeschke U, Karsten U, Reimer T, et al. Stimulation of hCG protein and mRNA in first trimester villous cytotrophoblast cells in vitro by glycodelin A. J Perinat Med. 2005; 33:212–218. [PubMed: 15914343]
50. Julkunen M, Rutanen EM, Koskimies A, et al. Distribution of placental protein 14 in tissues and body fluids during pregnancy. Br J Obstet Gynaecol. 1985; 92:1145–1151. [PubMed: 4063232]
51. Gabay C, Kushner I. Acute-phase proteins and other systemic responses to inflammation. N Engl J Med. 1999; 340:448–454. [PubMed: 9971870]
52. Oh SK, Leung MF, Knee T, et al. Biological properties of suppressive E-receptor factor on lymphokine function. Eur J Immunol. 1987; 17:1403–1409. [PubMed: 3119348]
53. Arredouani M, Matthijs P, Van Hoeyveld E, et al. Haptoglobin directly affects T cells and suppresses T helper cell type 2 cytokine release. Immunology. 2003; 108:144–151. [PubMed: 12562322]
54. Baseler MW, Burrell R. Purification of haptoglobin and its effects on lymphocyte and alveolar macrophage responses. Inflammation. 1983; 7:387–400. [PubMed: 6654476]
55. Oh SK, Ross S, Walker J, et al. Role of a SER immune suppressor in immune surveillance. Immunology. 1988; 64:73–79. [PubMed: 3260218]
56. Maffei M, Funicello M, Vottari T, et al. The obesity and inflammatory marker haptoglobin attracts monocytes via interaction with chemokine (C-C motif) receptor 2 (CCR2). BMC Biol. 2009; 7:87. [PubMed: 20017911]
57. Andrews WW, Goldenberg RL, Faye-Petersen O, et al. The Alabama Preterm Birth study: polymorphonuclear and mononuclear cell placental infiltrations, other markers of inflammation, and outcomes in 23- to 32-week preterm newborn infants. Am J Obstet Gynecol. 2006; 195:803–808. [PubMed: 16949415]

NIH-PA Author Manuscript

NIH-PA Author Manuscript

NIH-PA Author Manuscript

58. Kim MJ, Romero R, Gervasi MT, et al. Widespread microbial invasion of the chorioamniotic membranes is a consequence and not a cause of intra-amniotic infection. Lab Invest. 2009; 89:924–936. [PubMed: 19506551]

59. Soni C, Karande AA. Glycodelin A suppresses the cytolytic activity of CD8+ T lymphocytes. Mol Immunol. 2010; 47:2458–2466. [PubMed: 20638131]

NIH-PA Author Manuscript
NIH-PA Author Manuscript
NIH-PA Author Manuscript

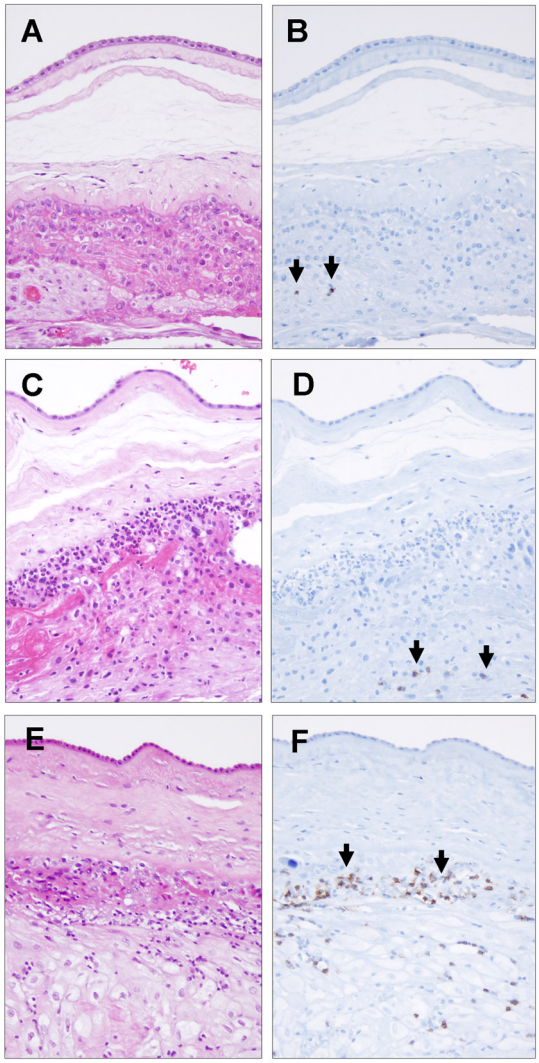

Figure 1.
Pathologic characteristics of acute and chronic chorioamnionitis. (A, B) Histological findings of a preterm labor case without inflammation, showing no evidence of extrinsic infiltrates (A). Few CD8+ T cells (arrows) are found in the decidua (B). (C, D) A case of acute chorioamnionitis showing characteristic amniotropic neutrophil infiltration into the chorionic connective tissue layer (C). CD8+ T cells (arrows) are restricted to the decidual layer (D). (E, F) A case of chronic chorioamnionitis with infiltration of lymphohistiocytes into the chorionic trophoblast layer (E), which are predominantly of CD8+ T cells (arrows) (F). Original magnification (A–F), X200.

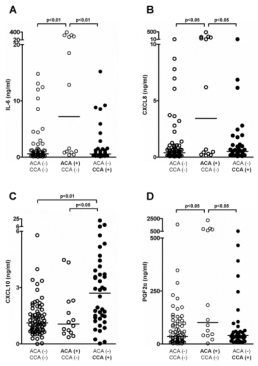

Figure 2.

Differences in amniotic fluid IL-6, CXCL8, CXCL10, and $PGF_{2\alpha}$ concentrations according to the type of inflammation in preterm labor cases (n=125). (A, B) Amniotic fluid IL-6 and CXCL8 concentrations are elevated in cases of acute but not chronic chorioamnionitis. (C) Amniotic fluid CXCL10 concentration is elevated in cases of chronic but not acute chorioamnionitis. (D) Amniotic fluid $PGF_{2\alpha}$ concentration in each group, showing an elevation in acute chorioamnionitis cases compared to other groups. ACA: acute chorioamnionitis, CCA: chronic chorioamnionitis.

NIH-PA Author Manuscript NIH-PA Author Manuscript NIH-PA Author Manuscript

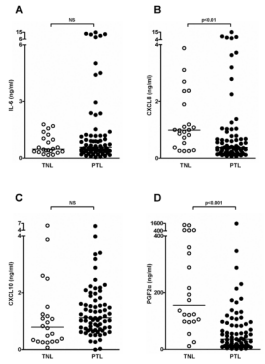

Figure 3.

Amniotic fluid IL-6 (A), CXCL8 (B), CXCL10 (C), and $PGF_{2\alpha}$ (D) concentrations in preterm labor cases without inflammation (n=71) and term not in labor cases (n=22). Amniotic fluid CXCL8 and $PGF_{2\alpha}$ concentrations are significantly higher in term not in labor cases than in preterm labor cases ($p<0.01$ and $p<0.001$, respectively), whereas there is no difference in IL-6 and CXCL10 concentrations. PTL: preterm labor, TNL: term not in labor.

NIH-PA Author Manuscript
NIH-PA Author Manuscript
NIH-PA Author Manuscript

NIH-PA Author Manuscript

NIH-PA Author Manuscript

NIH-PA Author Manuscript

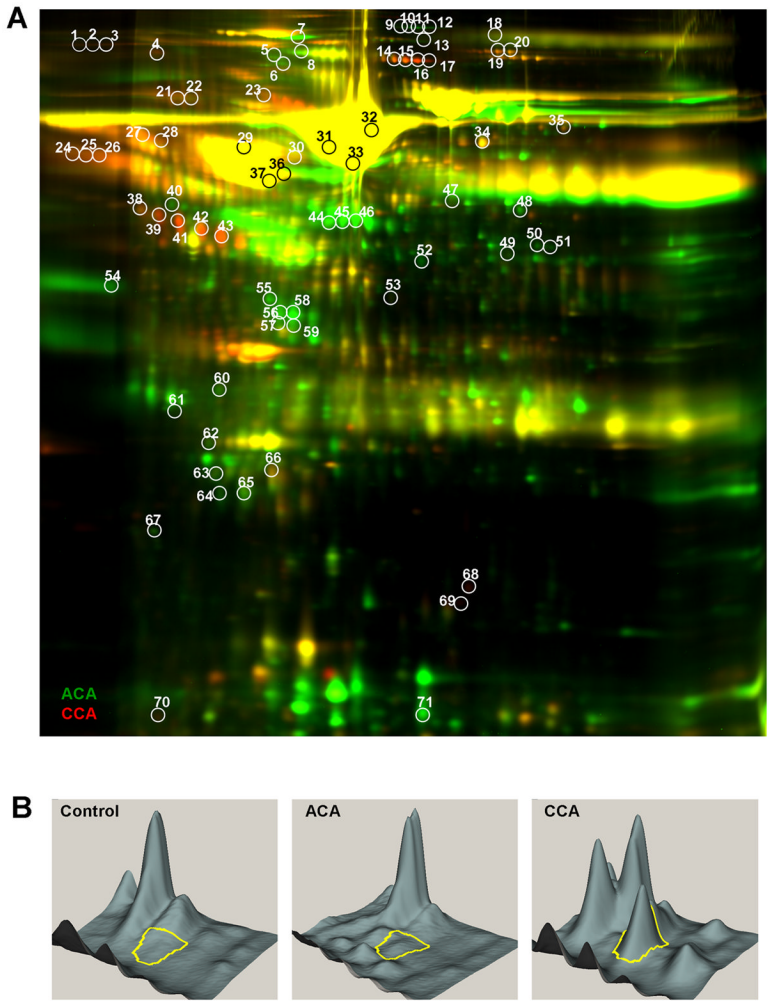

Figure 4.

Identification of differentially abundant proteins in amniotic fluid samples from chronic chorioamnionitis cases. (A) Two-dimensional difference in gel electrophoresis (2D-DIGE) images showing differentially expressed proteins between acute chorioamnionitis cases (Cy3: green) and chronic chorioamnionitis cases (Cy5: red). The spots are labeled by number. (B) Three-dimensional images from DeCyder software analysis for spot 42 marked in the 2D-DIGE image (A), which is increased in chronic chorioamnionitis. The spot was identified as β-haptoglobin by MALDI-TOF-MS/MS. ACA: acute chorioamnionitis, CCA: chronic chorioamnionitis.

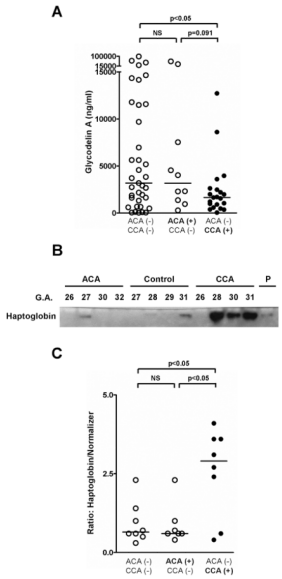

Figure 5.

Differential abundance of glycodelin-A and β-haptoglobin in chronic chorioamnionitis cases with gestational ages of 32 weeks or less. (A) Amniotic fluid glycodelin-A concentration is significantly lower in chronic chorioamnionitis cases (n=21) compared to that of control cases (n=37) and acute chorioamnionitis cases (n=10). (B) Immunoblotting results showing increased abundance of β-haptoglobin subunit in chronic chorioamnionitis cases. Amniotic fluid (3.5 μl) was electrophoresed in 12% SDS-PAGE under reducing conditions. P: a pooled amniotic fluid sample as a normalizer in densitometric analysis. (C) The results of densitometric analysis of β-haptoglobin immunoblotting. Haptoglobin is significantly increased in the amniotic fluid of chronic chorioamnionitis cases (n=8) compared to control cases (n=8) and to acute chorioamnionitis cases (n=7). The graph depicts the relative density of each sample using the density of a pooled amniotic fluid sample as a normalizer. ACA: acute chorioamnionitis, CCA: chronic chorioamnionitis.

NIH-PA Author Manuscript NIH-PA Author Manuscript NIH-PA Author Manuscript

NIH-PA Author Manuscript
NIH-PA Author Manuscript
NIH-PA Author Manuscript

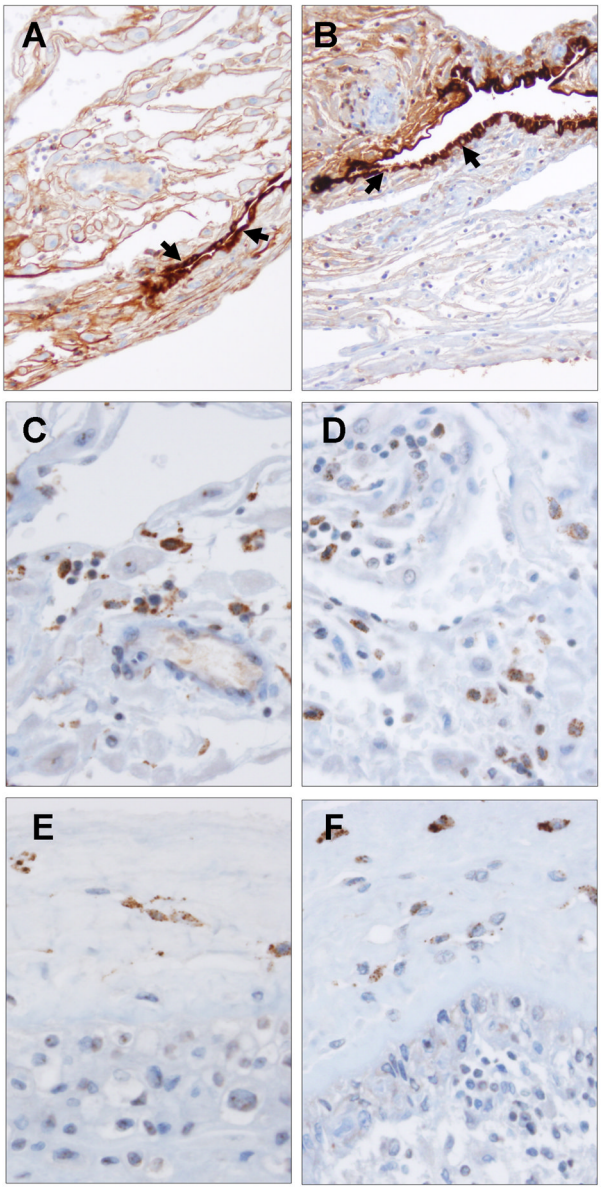

Figure 6.

Immunoreactivity of glycodelin-A and haptoglobin in the chorioamniotic membranes. (A) Distinct glycodelin-A immunoreactivity in the endometrial epithelial cytoplasm (arrows) in a preterm labor case without inflammation. Membranous immunoreactivity is far more prominent in the decidual stromal cells. (B) A chronic chorioamnionitis case showing similar immunoreactive patterns in the endometrial epithelial cytoplasm (arrows). (C–F) Coarsely granular haptoglobin immunoreactivity is mainly found in decidual leukocytes and in myofibroblasts (C) and macrophages of the chorionic connective tissue from a preterm labor case without inflammation (E). Similar immunoreactive patterns also found in a chronic chorioamnionitis case. Decidual leukocytes (D) and myofibroblasts and macrophages in the chorionic connective tissue (F). Original magnification (A, B), X200; (C–F), X400.

NIH-PA Author Manuscript

NIH-PA Author Manuscript

NIH-PA Author Manuscript

Table 1

Demographic and clinical characteristics of the study population

	ACA−/CCA− (n=71)	ACA+/CCA− (n=14)	ACA−/CCA+ (n=40)
Maternal age (years)	23.5 (±5.7)	24.3 (±8.9)	24.7 (±6.6)
Nulliparous	31 (43.7%)	8 (57.1%)	15 (37.5%)
GA at amniotic fluid sampling (weeks)	31.0 (±3.0)	29.8 (±3.5)	31.4 (±2.8)
GA at delivery (weeks)†	36.5 (±2.9)	32.9 (±5.5)*	35.4 (±3.7)
Interval amniocentesis-delivery (days) †	38.2 (±28.5)	22.0 (±24.9)	28.3 (±23.6)
Birth weight (grams) †	2753.7 (±712.7)	2155.0 (±1125.2)**	2548.3 (±844.1)
Birth weight <10th percentile	11 (15.5%)	1 (7.1%)	7 (17.5%)

Data are presented as mean (±SD) or number (percentage)

† p <0.05 among three groups

* p <0.05 compared to ACA−/CCA−

** p <0.05 compared to both ACA-/CCA− and ACA−/CCA−

ACA: acute chorioamnionitis, CCA: chronic chorioamnionitis, GA: gestational age.

NIH-PA Author Manuscript

NIH-PA Author Manuscript

NIH-PA Author Manuscript

Table 2

Amniotic fluid peptides showing significant changes with chronic chorioamnionitis cases compared to acute chorioamnionitis cases or cases without chorioamnionitis

Spot number	Protein name	Accession number	MW (Da)	Protein PI
4	Proteoglycan 2 preproprotein	gi|46276889	25189.3	6.3
7	Ceruloplasmin	gi|1620909	115398.4	5.4
8	Albumin preproprotein	gi|4502027	69321.5	5.9
10	Serum albumin precursor	gi|6013427	69180.4	5.9
13	Complement component 6	gi|38488662	104739.1	6.4
15	Complement factor B	gi|13278732	85508.5	6.6
19	Plasminogen	gi|4505881	90510.2	7.0
22	Transferrin	gi|115394517	76909.6	7.0
25	Alpha-2-HS-glycoprotein	gi|156523970	39315.7	5.4
27	Alpha-1-antichymotrypsin precursor	gi|177933	45453.4	5.3
28	Kininogen 1 variant	gi|62898910	47822.6	6.3
29	Alpha-1 antitrypsin variant	gi|110350939	46577.0	5.4
30	Chain A, the intact and cleaved human antithrombin III complex	gi|999513	49008.0	6.0
32	Chain A, structure of human serum albumin with S-Naproxen and the Ga module	gi|168988718	65777.6	5.6
36	Vitamin D-binding protein/group specific component	gi|455970	52916.0	5.3
40	Chain A, crystal structure of a Serpin:protease complex	gi|11514321	37624.4	5.3
42	Haptoglobin	gi|3337390	38209.2	6.1
45	PRO2619	gi|11493459	56745.2	6.0
47	Hemopexin, isoform CRA_d	gi|119589127	43201.2	6.2
48	Phosphogluconate dehydrogenase	gi|40068518	53105.9	6.8
49	Enolase 1 variant	gi|62897945	47167.3	7.0
52	Albumin-like	gi|763431	52047.8	5.7
55	Leucine-rich alpha-2-glycoprotein 1	gi|16418467	38154.1	6.5
61	Progestagen-associated endometrial protein	gi|55958594	14792.5	5.2
62	Chain A, crystal structure of lipid-free human apolipoprotein A-I	gi|90108664	28061.5	5.3
63	Orosomucoid 2	gi|48145977	23599.7	5.0
64	Chain A, crystal structure of the trigonal form of human plasma retinol-binding protein	gi|157830446	20945.1	5.3
65	Chain E, crystal structure of the transthyretin-retinol binding protein-Fab complex	gi|212374946	20189.7	5.1
67	Insulin-like growth factor binding protein 1 precursor	gi|4504615	27885.3	5.1
68	Chain B, structural basis for the inhibition of insulin-like growth factors by Igf binding proteins	gi|114793741	9808.5	5.3
71	Albumin, isoform CRA_p	gi|119626079	22498.5	8.2

Spot numbers shown in 2D-DIGE image (Figure 2A).